PCCP

Accepted Manuscript

ROYAL SOCIETY OF CHEMISTRY

www.rsc.org/pccp

Unequal effect of ethanol/water on the stability of ct-DNA, poly [(dA-dT)] $_2$ and poly(rA)·poly(rU). Thermophysical properties†

Rebeca Ruiz,[a] Francisco J. Hoyuelos,[a] Ana M. Navarro,[a] José M. Leal[a] and Begoña García,*[a]

[a]Universidad de Burgos, Departamento de Química, 09001 Burgos, Spain.

*Corresponding Author: begar@ubu.es

Abstract

Ethanol affects unequally the thermal stability of DNA and RNA. It stabilizes RNA, while destabilizing DNA. The variation with temperature of the relative viscosity (η/η_0) of [poly(dA-dT)]$_2$ unveils transitions close to the respective denaturation temperature, calculated spectrophotometrically and calorimetrically. From the raw data densities and speeds of sound, the volumetric observables were calculated. In all cases studied, a change in sign from low to high ethanol content occurred for both partial molar volume (ϕV) and partial molar adiabatic compressibility (ϕK_S). The minima, close to 10%, should correspond to highest solvation and the maxima, close to 30%, to lowest solvation. For 40-50% ethanol, the solvation increases again. The complex structure of ethanol/water, for which changes are observed in regions close to such critical concentrations, justifies the observed behviour. The variation of ϕV and ϕK_S was sharper for RNA compared to DNA, indicating that the solvation sequence is poly(rA)·poly(rU) < ct-DNA < [poly(dA-dT)]$_2$.

Keywords: DNA, RNA, thermal stability, thermophysical properties, ethanol-water

1. Introduction

Water is an integral part of DNA. Solvation exerts control over the specificity of proteins and their binding to DNA,[1] as double-stranded DNAs are surrounded by at least two solvation layers.[2] The form adopted by the helical structure of DNA is determined essentially by the activity of water and the nature of the ions in solution.[3] The factors that exert control of the binding of drugs to DNA can afford valuable information but, despite the efforts in this direction, the interaction of DNA with the solvent still remains unclear.[4-9]

Mixed solvents are used in equilibrium, kinetic and biological studies.[10-12] Since the first reports about the effect of ethanol-water on the optical and hydrodynamic parameters of DNA,[13,14] the effect of ethanol on the structure,[15-18] stability[19] and conformation[15,20] of DNA have attracted growing interest. Small amounts of ethanol can distort DNA without modifying its conformation; however, if ethanol approaches 50% (v/v), aggregation and precipitation of B-DNA happens,[15] and above 70% (v/v), the B→A[20] and B→C[21] transitions are likely to occur. In the absence of ethanol, the volumetric properties of nucleic acids depend on the base sequence;[22-24] hence, the effect of ethanol/water mixtures on the conformational stability of nucleic acids seems linked to solvent properties.[25]

In this work, the stability and solvation features of the ct-DNA and $[poly(dAdT)]_2$ forms of B-DNA and the poly(rA)·poly(rU) form of A-RNA have been studied in ethanol/water mixtures up to 40-50% (ethanol mole fraction, x = 0.17-0.24). Small amounts of ethanol destabilize the B-DNA double helix, while that of A-RNA becomes stabilized, an issue not reported hitherto. The volumetric properties of RNA and DNA depend on the polynucleotide conformation, the base type and the solvent mixture and were measured at neutral pH as a function of temperature and ethanol content by means of acoustic, densitometric and viscometric measurements. The observable properties expansibility, relative molar speed of sound, adiabatic isentropic compressibility, partial molar volume and partial molar adiabatic compressibility, along with differential scanning calorimetry, circular

dichroism and viscometry measurements have provided new insights into the solvation features of the nucleic acids studied.

2. Materials and methods

2.1 Materials

Calf thymus DNA (ct-DNA), $[poly(dA\text{-}dT)]_2$ and poly(rA)·poly(rU), of the highest purity commercially available (Sigma-Aldrich), were used without further purification; the C_P concentrations, given as molar base-pairs (M_{BP}), were calculated from their respective absorptivities: ct-DNA (ε_{260nm} = 13200 $M^{-1}cm^{-1}$),[26] $[poly(dA\text{-}dT)]_2$ (ε_{260nm} = 13300 $M^{-1}cm^{-1}$)[27] and poly(rA)·poly(rU) (ε_{260nm} = 14900 $M^{-1}cm^{-1}$) at *pH* = 7 and *I* = 0.1 M. Stock solutions of the polynucleotides were prepared with doubly distilled water in 0.1 M NaCl, maintaining the *pH* constant at 7.0 with sodium cacodylate [$(CH_3)_2AsO_2Na$]; the concentrations were determined from their absorptivities. Working solutions were prepared by adding to aliquots of the stock solutions the amounts of water and ethanol needed to reach the required solvent composition. The C_P values were corrected for every ethanol concentration considering the negative excess volume (ΔV^E) of the ethanol-water mixtures.[28] The maximum degree of uncertainty in the C_P measurements was $\pm 2 \times 10^{-5} M_{BP}$.

2.2 Methods

The values of *pH* were taken with a Metrohm pH meter (Herisau, Switzerland) and a Biotrode Metrohm glass electrode with 3 M KCl liquid junction, correcting the readings for ethanol-water mixtures as::[29] $pH = pH_{read} - \delta$, being *w* the ethanol/water (*w*/*w*) content and $\delta = 9.48 \cdot 10^{-2} - 1.16 \cdot 10^{-2} \cdot w + 5.19 \cdot 10^{-4} \cdot w^2 - 5.86 \cdot 10^{-6} \cdot w^3 - 1.88 \cdot 10^{-8} \cdot w^4$.

The spectrophotometric study of thermal denaturation was conducted by heating the polynucleotide samples ($C_P = 4 \times 10^{-5}$ M_{BP}) from 20 to 90 °C at 0.25 °C/min scan rate and recording the absorbance readings with a Hewlett-Packard 8453A photodiode array

spectrophotometer (±0.5 nm, Agilent Technologies, Palo Alto, California) fitted out with a HP-89090 Peltier temperature control system, (±0.1 °C).

The thermal behaviour was also studied by DSC measurements, with a Nano DSC Instrument (TA, Waters LLC, New Castle, USA). To reduce to a minimum the formation of bubbles upon heating, the reference and sample solutions were degassed in a degassing station (TA, Waters LLC, New Castle, USA). The samples with polynucleotide concentration C_P = 5 × 10^{-4} M_{BP} were scanned at 1 atm pressure from 20 to 90°C at 1 °C·min^{-1} scan rate for ct-DNA and poly(rA)·poly(rU) and 0.25 °C·min^{-1} for [poly(dA-dT)]$_2$. The integration area of the surface covered by the calorimetric curve between two temperatures, T_1 and T_2, has allowed us to calculate the ΔH^0_{cal} and ΔS^0_{cal} values according to:

$$\Delta H^0_{cal} = \int_{T_1}^{T_2} C_P \, dT \qquad \text{and} \qquad \Delta S^0_{cal} = \int_{T_1}^{T_2} \left(\frac{C_P}{T} \right) dT \tag{1}$$

The C_P = f (T) data were analyzed using the built-in software "NanoAnalyze Data Analysis, version 2.3.6 Copyright (C) 2005, 2011 TA Instruments DSC".

Circular dichroism (CD) measurements were taken with a MOS-450 spectrophotometer (Bio-Logic SAS, Claix, France) using a Xenon Arc lamp. The cell temperature was controlled by an external Julabo bath (± l ºC). Spectral curves in the 200−400 nm range were recorded at 5 nm/s and polynucleotide concentration C_P = 5×10^{-5} M_{BP}. The molar ellipticities (degM_{BP}^{-1}cm^{-1}) were calculated using [θ] = 100 $\theta/C_P l$, with l being the cell light path (cm).

Densities (ρ) and speeds of sound (u) were measured in the 25-65 ºC range with an Anton Paar DSA 5000 oscillating U-tube densitometer (Graz, Austria). The density readings (± 5×10^{-6} g cm^{-3}), based on the oscillation period of the sample tube, and the speeds of sound (± 0.5 m s^{-1}) were obtained from the traveling time of an electrical impulse emitted by a piezoelectric element. Proper calibration at each temperature (± 0.01 ºC) was achieved with doubly distilled water (Milli-Q, Millipore) and n-nonane (Fluka, 99.2%) as standards. The scan rate was 0.1 ºC/min and the polynucleotide concentration was C_P = 5×10^{-4} M_{BP}.

Dynamic viscosities (η, ± 5×10^{-3} mPa s) were measured with an automated Anton Paar AMV200 viscometer (Graz, Austria), calibrated with doubly distilled water (Milli-Q, Millipore). The viscosity values, based on the rolling ball principle, were obtained measuring the shear stress of a steel ball introduced into an inclined, sample-filled glass capillary, inside a thermostatic block; the temperature (± 0.01 ºC), controlled by an external F25 Julabo bath (Seelbach, Germany), was measured with a Pt100 *Guildline* 9890 thermometer. The stress was monitored switching the inclination angle within 20-80°. The dynamic viscosities were evaluated as: $\eta = k(\alpha)\cdot t\cdot(\rho_{ball} - \rho)$, $k(\alpha)$ being the calibration constant at each inclination angle and temperature, t (± 0.01 s) stands for the rolling time, ρ_{ball} for the density of the ball (7.85 g cm^{-3}) and ρ for the solution density. Viscosities were measured between 25-65 ºC for $C_P = 5\times10^{-4}$ M_{BP}.

3. Results and Discussion

Fig. 1S (ESI†) collects the UV-Vis spectra in the 220-340 nm range for solutions of ct-DNA, $[poly(dA\text{-}dT)]_2$ and poly(rA)·poly(rU) between 0 and 70% (v/v) ethanol, I = 0.1 M (NaCl), pH = 7.0 and T = 25 ºC. Fig. 1A shows the absorbance at λ = 260 nm and Fig. 1B the λ_{max} shift of the three systems as a function of the ethanol concentration.

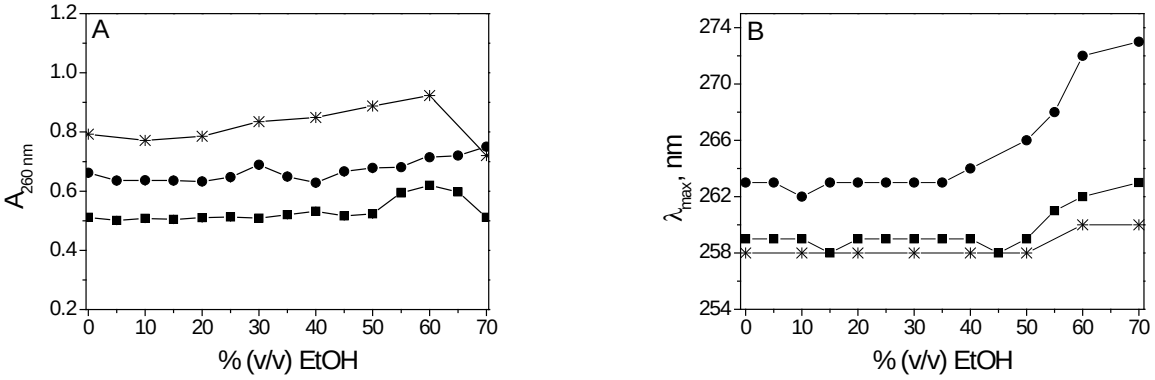

Fig. 1 (A) Variation of absorbance at λ = 260 nm. (B) shift of λ_{max} as a function of ethanol concentration: (■) ct−DNA, (●) $[poly(dA-dT)]_2$, (∗) poly(rA)·poly(rU). $C_P = 5\times10^{-5}$ M_{BP}, I = 0.1 M (NaCl), pH = 7.0, T = 25 ºC.

The CD spectra for all of the three systems are collected in Fig. 2S (ESI†). The isoelliptic points (Fig. 2SA and 2SC, ESI†) recorded up to 50% (v/v) for ct-DNA (300 nm) and poly(rA)·poly(rU) (275 nm) unveil equilibria between two conformations; $[poly(dA\text{-}dT)]_2$ displayed no isoelliptic point (Fig. 2SB, ESI†). The CD spectra recorded up to 40% (v/v) for the three polynucleotides displayed no conformational change at 260 nm (Fig. 2A), but a notable gap emerged around 50% (v/v). This behaviour is also observed in Fig. 2B, showing the shift of the maxima when the ethanol content varies; the structural changes observed for ct-DNA and $[poly(dA\text{-}dT)]_2$ reflect the transition from conformation B (0-40% (v/v)) to A (70% (v/v)),[19,20,30] while poly(rA)·poly(rU) adopts the A conformation.[31]

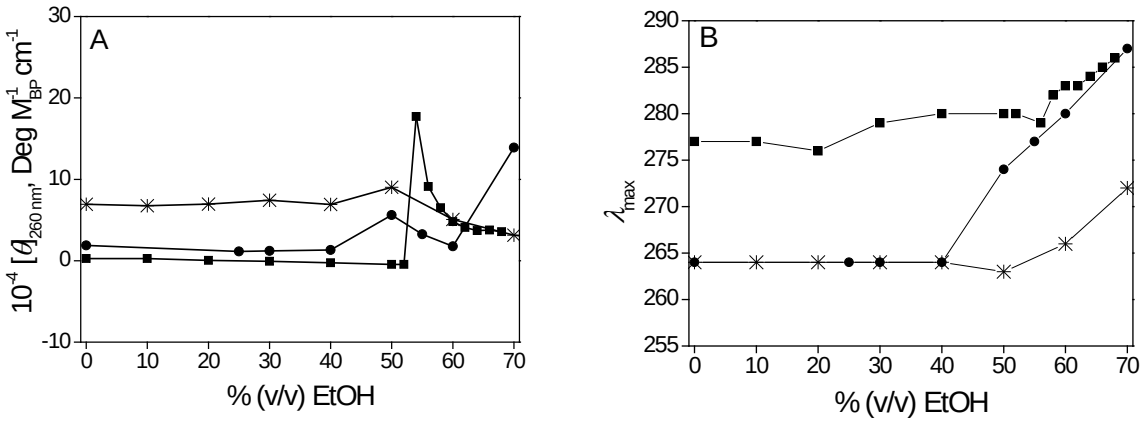

Fig. 2 (A) Variation of molar ellipticity [θ] at λ = 260 nm as a function of ethanol content (v/v); B) shift of the maximum molar ellipticity as a function of ethanol content, (■) ct-DNA, (●) $[poly(dA\text{-}dT)]_2$ and (∗) poly(rA)·poly(rU). $C_P = 5\times10^{-5}$ M_{BP}, I = 0.1 M (NaCl), pH = 7.0, T = 25 ºC.

3.1. Thermal denaturation

The thermal stability of poly(rA)·poly(rU) and $[poly(dA\text{-}dT)]_2$ was monitored by UV-Vis and DSC measurements within the 0-40% (v/v) range and for ct-DNA within 0-50%, the ranges in which the CD spectral curves did not change appreciably (Figure 2). For denaturation of double helix, A_2, into single strands, A:

$$A_2 \underset{}{\overset{K_d}{\rightleftharpoons}} 2\ A \qquad (2)$$

the fraction α of single strand is defined as:

$$\alpha = \frac{A - A_D}{A_S - A_D} \tag{3}$$

where A_D, A_S and A stand for the absorbance of double helix, single helix and varying absorbance, respectively. The α versus T plot yielded sigmoid curves (Fig. 3S, ESI†). The melting temperature, $T_{m,sp}$, was evaluated as the intersection between the two baselines and the absorbance curve.[32]

The calorimetric denaturation curves for all of the three systems were recorded using the same solvents Fig. 4S (ESI†). The temperature of maximum heat capacity, C_p, was taken as the calorimetric denaturation temperature ($T_{m,cal}$). Table 1 lists the ΔH^0_{cal} and ΔS^0_{cal} values for ct-DNA, $[poly(dA\text{-}dT)]_2$ and poly(rA)·poly(rU) calculated with eqn 1 for each ethanol concentration; for ct-DNA, these quantities could not be obatined for 0 and 10% because the high T_m required gave unfinished calorimetric curves at 90ºC, the highest working temperature attainable at P = 1atm (see Fig. 4S, (ESI†).

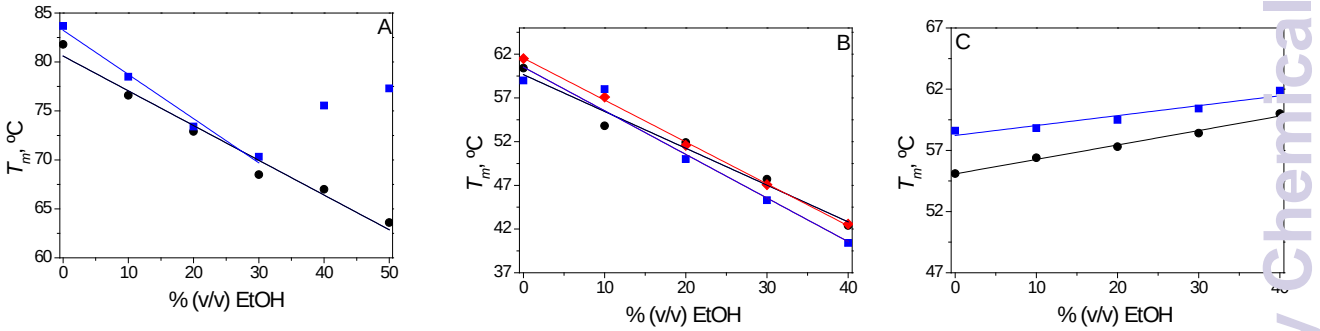

Figure 3 Least-square fitting of T_m as a function of ethanol content for (A) ct-DNA, (B) $[poly(dA\text{-}dT)]_2$ and (C) poly(rA)·poly(rU). (●) $T_{m,sp}$ $C_P = 4\times10^{-5}$ M_{BP} (◆) $T_{m,vis}$ and (■) $T_{m,cal}$. $C_P = 5\times10^{-4}$ M_{BP}, I = 0.1 M (NaCl), pH = 7.0.

Fig. 3 plots the spectrophotometric ($T_{m,sp}$) and calorimetric ($T_{m,cal}$) values obtained. For ct-DNA, $T_{m,sp}$ yielded a straight line plot with negative slope (-0.355) over the whole composition range (Fig. 3A), while $T_{m,cal}$ varied linearly only up to 30%, with slightly larger negative slope (-0.451). For DNA, a notable difference between the $T_{m,cal}$ and $T_{m,sp}$ values was observed at 40 and 50% ethanol because $T_{m,cal}$ increased while $T_{m,sp}$ decreased. The increase in $T_{m,cal}$ could be due to the tendency of B-DNA to self-aggregate approaching 40%

(v/v), as conformational changes for these ethanol levels were absent (Figs. 1 and 2). As to the melting effects, the only difference between the spectrophotometric (Fig. 3SA, ESI) and calorimetric (Fig. 4SA, ESI) procedures lies in the different working concentration demanded by the UV-Vis and DSC techniques (roughly 10-fold increase for DSC relative to UV) and the scan rates employed, 0.25ºC/min and 1.0ºC/min for UV and DSC, respectively. An adequate DSC analysis for ct-DNA and poly(rA)·poly(rU) was not viable at 0.25ºC/min because the curves were rather smooth and the resulting $T_{m,\mathrm{cal}}$ value was imprecise.

Denaturation experiments performed with ct-DNA and poly(rA)·poly(rU) at λ = 260 nm between 0.2 and 1ºC/min have shown that $T_{m,sp}$ is independent of the scan rate (Fig. 5S(ESI†). Thus, the kinetic processes (disaggregation and melting) are related to the type and concentration of the polynucloetide.[33] For $[poly(dA\text{-}dT)]_2$, $T_{m,sp}$ and $T_{m,cal}$ were quite similar (also coincident with the viscosity reading, $T_{m,vis}$, Fig. 3B) whose negative slope (~ -0.48) indicates that ethanol destabilizes $[poly(dA\text{-}dT)]_2$. For this system, the DSC and UV–Vis measurements could be conducted at low scan rate, thereby the T_m values from the three different sources were closer compared to the other two systems. For poly(rA)·poly(rU), the slope was always positive with $T_{m,cal}$ (0.081) and $T_{m,sp}$ (0.118) (Fig. 3C). The observed increase in T_m for poly(rA)·poly(rU) upon increasing ethanol (Table 1) can be explained by the formation of thermally stable A-RNA fibers, which may result in condensation. The 2-3 ºC difference between both melting temperatures is ascribable to concentration effects.

The electrostatic interactions become stronger as the solvent permittivity (ε) decreases, thus enhancing the condensation of the counterion and facilitating the aggregation to neighbour polynucleotide units. With DNA, this effect was observable only for ct-DNA above the 40% critical limit, far from the 70-80% reported.[34] The modest solvatochromic and conformational changes displayed up to 40% ethanol (Figs. 1B and 2B) exclude solvent-induced structural changes. The noticeable differences found have been attributed to the GC content for ethanol concentrations 65% and above in the dynamics of the B-A transition of

DNA and $[poly(dA\text{-}dT)]_2$;[35] it can be assumed that the GC content of ct-DNA also is responsible for the different activity of water, which promotes aggregation of ct-DNA from 40% ethanol, whereas no aggregation phenomena were observed with $[poly(dA\text{-}dT)]_2$ under the same experimental conditions. The effects described so far reveal the pronounced dependence of T_m on the nucleic acid (DNA or RNA), the polynucleotide concentration, the ethanol content and the base type. Hence, it is not fully right to link the prevailing denaturation mechanism to solely the solvent properties.[22,36]

The denaturation enthalpies ΔH^0_{cal} for ct-DNA and poly(rA)·poly(rU) are smaller compared to those of $[poly(dA\text{-}dT)]_2$; the entropies followed the sequence poly(rA)·poly(rU) < ct-DNA < $[poly(dA\text{-}dT)]_2$ (Table 1). For ct-DNA, the entropy clearly diminished for 40 and 50% ethanol compared to 20 and 30%. This behaviour apparently comes into conflict with occurence of aggregates, whose disaggregation would contribute to positive entropy. However, the solvation processes contribute more importantly, as will be shown below with

Table 1 Spectrophotometric melting temperature ($T_{m,sp}$) and DSC thermodynamic parameters ($T_{m,cal}$, ΔH^0_{cal} and ΔS^0_{cal}) for ct-DNA, $[poly(dA\text{-}dT)]_2$ and poly(rA)·poly(rU) and melting temperature from viscosity measurements ($T_{m,vis}$) for $[poly(dA\text{-}dT)]_2$. I = 0.1 M (NaCl), pH = 7.0.

	%(v/v) EtOH	$T_{m,sp}$ (°C)	$T_{m,cal}$ (°C)	ΔH^0_{cal} (kJ mol^{-1})	ΔS^0_{cal} (J mol^{-1} K^{-1})	$T_{m,vis}$ (°C)
ct-DNA	0	81.8	83.7			
	10	76.6	78.5			
	20	72.9	73.4	34.4	99.3	
	30	68.5	70.3	30.7	95.3	
	40	67.0	75.5	20.5	58.8	
	50	63.6	77.3	18.2	51.9	
$[poly(dA\text{-}dT)]_2$	0	60.4	61.5	37.3	112	59.0
	10	53.8	57.1	42.7	129	58.0
	20	51.9	51.6	48.2	154	50.0
	30	47.7	47.1	47.8	158	45.3
	40	42.4	42.6	36.6	122	40.4
poly(rA)·poly (rU)	0	55.1	58.6	31.2	87.5	
	10	56.4	58.8	30.0	85.8	
	20	57.3	59.5	28.9	87.4	
	30	58.4	60.4	29.7	89.9	
	40	60.0	61.9	27.7	83.7	

the thermophysical properties. The solvation of ctDNA is greater for 40 and 50% ethanol than for 20 and 30%, which justifies the ΔS^0 values obtained. Therefore, the observed changes in the thermal stability should not be exploited as dependent only on the solvent structure and the A or B conformation as they, in fact, reflect a variety of interactions and are affected by coupled processes from both the solvent and the nucleic acids in different conformations.

3.2. Thermophysical Properties

Density and speed of sound. For ct-DNA, [poly(dA-dT)]$_2$ and poly(rA)·poly(rU) these properties were measured as a function of temperature and ethanol concentration. Table S1 (ESI†) lists the ρ_0 and u_0 values for the solvent between 0-50% v/v ethanol in the 25-65 ºC range. Tables S2 to S20 (ESI†) list the ρ and u values from 25 to 65 ºC, between 0-40% v/v ethanol for [poly(dA-dT)]$_2$ and poly(rA)·poly(rU), and 0-50% v/v for ct-DNA; conformational changes were absent. From the values of ρ and u, the following useful derived properties were calculated:

Cubic expansion coefficient, $$\alpha = -1/\rho \cdot \left(\delta\rho/\delta T\right)_P \quad (4)$$

Relative molar speed of sound, $$[U] = \frac{u - u_0}{u_0 \cdot C_P} \quad (5)$$

Isentropic compressibility, $$K_S = \frac{1}{u^2 \rho} \quad (6)$$

Partial molar volume,[37] $$\phi V = \left(M/\rho_0\right) - \left(\rho - \rho_0\right)/\rho_0 \cdot C_P \quad (7)$$

that is, the apparent volume occupied by one mole of solute at infinite dilution,[23] M being the molar weight.

Partial molar adiabatic compressibility ϕK_S, defined as:[38]

$$\phi K_S = \beta_{S0}\left(2\phi V - 2[U] - M/\rho_0\right) \quad (8)$$

where β_{S0} is the solvent coefficient of adiabatic compressibility. The errors percentage, estimated adding the maximum uncertainty in concentration, temperature drift and

instrumental limitation, were calculated as: ± 1.61% for [U], ± 2.62% for ϕV, ±2.14% for ϕK_S, ±0.05% for α, ±0.36% for K_S and ±0.36% for β_{S0}.

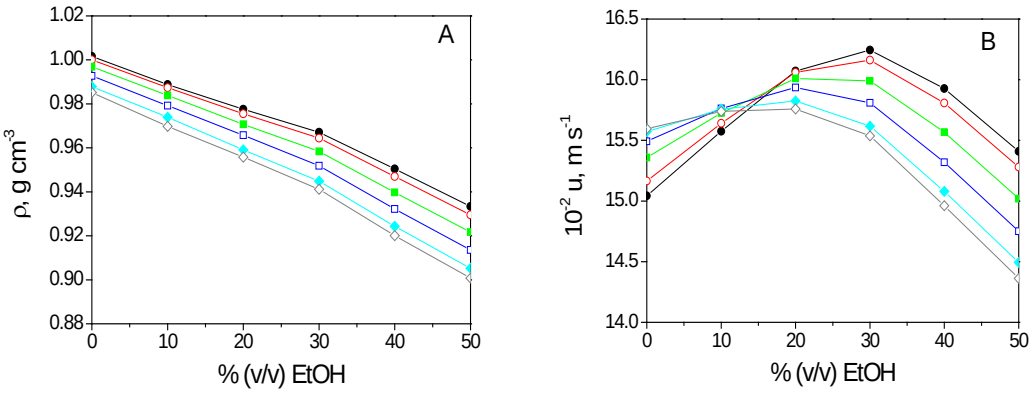

Fig. 4 (A) Density, ρ, and (B) speed of sound, u, for ct-DNA as a function of %(v/v) ethanol at different temperatures: (●)25, (○)30, (■)40, (□)50, (♦)60, (◊)65 ºC. $C_P = 5\times10^{-4}$ M_{BP}, I = 0.1 M (NaCl), pH = 7.0.

Fig. 4 plots the variation of ρ and u as a function of ethanol concentration for ct-DNA, the other systems behaving similar. The ρ values decreased when temperature and ethanol concentration increased (Fig. 4A) and u reached maxima at different ethanol contents depending on the temperature (Fig. 4B). A point of constant speed of sound was observed for ~15% ethanol; u increased when the temperature increased below this limit, whereas this variation reverted for higher ethanol content, at 25 ºC being highest; $[poly(dA\text{-}dT)]_2$ and poly(rA)·poly(rU) produced a similar pattern. Tables S2–S20 (ESI†) list the [U], ϕV, ϕK_S, α, K_S and β_{S0} values for all of the three polynucleotides.

Fig. 5 plots the observable properties α, [U], K_S, ϕV and ϕK_S as a function of ethanol concentration at different temperatures, calculated with eqns (4-8), (A) refers to ct-DNA, (B) to $[poly(dA\text{-}dT)]_2$ and (C) to poly(rA)·poly(rU). The coefficients of volume expansion, α, rose when the temperature and ethanol concentration were raised (Fig. 5(A1-C1)), consistent with the decrease in density under the same conditions. The relative molar speed of sound, [U], changed from positive to negative; at 20% (v/v), ct-DNA and $[poly(dA\text{-}dT)]_2$ displayed maxima, whose location shifted with the temperature, Figs. 5(A2-B2).

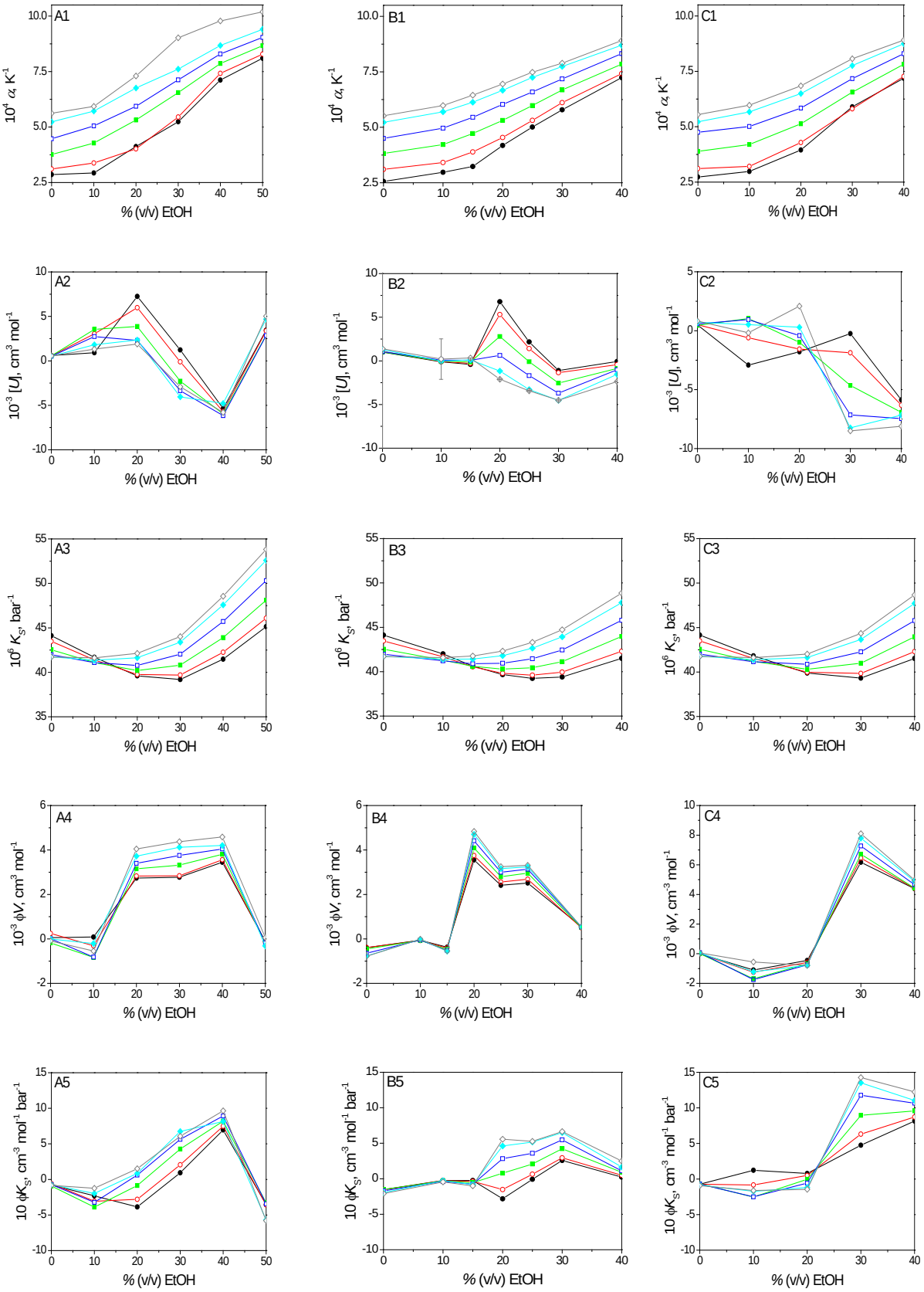

Fig. 5 (A1−C1), cubic expansion coefficient, α; (A2−C2), relative mixing molar speed of sound, [U]; (A3−C3), isentropic compressibility, K_S; (A4−C4), parcial molar volume, ϕV and (A5−C5) partial molar adiabatic compressibility, ϕK_S, as a function of %(v/v) ethanol: (●)25, (○)30, (■)40, (□)50, (♦)60, (◊)65 ºC. (A) ct-DNA, (B) [poly(dA-dT)]$_2$ and (C) poly(rA)·poly(rU). $C_P = 5\times10^{-4}$ M$_{BP}$, I = 0.1 M (NaCl), pH = 7.0.

Poly(rA)·poly(rU) showed a [*U*] temperature-independent point (≈ 22%) (Fig. 5C2). The variation of the isentropic compressibility, K_S, with temperature and solvent polarity, Fig. 5(A3-C3), reflects the variation of *u*, with a point of constant K_S at ≈ 15% (Fig. 4B). The minimum K_S value for 20−30% (v/v) ethanol corresponds to the maximum *u* value. Partial molar volume, ϕV, and partial molar adiabatic compressibility, ϕK_S, serve to measure the DNA-solvent interactions. Combination of density and speed of sound is sensitive to solvent interaction; thus, the variation of ϕV and ϕK_S bears relation to the number of surrounding solvent molecules, and is informative of solvation according to:[24]

$$\phi V = V_M + \Delta V_h \tag{9}$$

$$\phi K_S = K_M + \Delta K_{Sh} \tag{10}$$

where V_M and K_M (negligibly small for nucleic acids) stand for the intrinsic molar volume of the solute and intrinsic molar adiabatic compressibility, respectively; ΔV_h and ΔK_{Sh} account for the volume and compressibility solvation effects, respectively.[39] The ΔV_h contribution embodies two terms of opposite sign; the positive term is commensurate with the solute surface accessible to the solvent, and the negative one represents the diminution in the solvent volume due to H-bonding when the solvent gets access to polar or charged moieties.[39] Therefore, the larger the solvation effect (more polar groups exposed to solvent) the greater negative ΔV_h contribution. Fig. 5(A4-C4) shows the complex variation of ϕV with the ethanol concentration at different temperatures, stressing certain similarities that depend on the polynucleotide, which were nearly temperature independent. Up to 10% v/v, ϕV was close to zero regardless of the temperature, with maxima at 20% (v/v) for ct-DNA and $[poly(dA\text{-}dT)]_2$ and at 30% for poly(rA)·poly(rU).

Most of the atomic groups contribute negatively to ϕK_S. A large number of atomic groups exposed to solvent results in negative ΔK_{Sh} (eqn 10), yielding enhanced solvation. As

K_M was negligibly small for nucleic acids, the negative ϕK_S values reflect substantial solvation of nucleic acids. Fig. 5(A5-C5) shows that the partial molar adiabatic compressibility, ϕK_S, varied with the ethanol content for all temperatures. Up to 20% ethanol, the ϕK_S values remained nearly constant for all of the three systems. In addition, the ϕK_S values followed an unsteady trend with temperature.

The large ϕK_s and ϕV values for RNA (compared to DNA) denote that RNA becomes significantly less solvated,[40] an effect ascribable to the different structural features of the B and A duplexes rather than to the different chemical composition. In pure water, the counterions in the vicinity of poly(rA)·poly(rU) are significantly solvated, retaining only (34±21)% solvation sphere, whereas those in the vicinity of DNA are fully solvated.[41] Density and acoustic measurements have revealed the water contraction of 2-deoxyribose around polar groups to be 15–20% weaker than around polar ribose groups.[42] In all of the cases studied in this work, a change in sign from low to high ethanol content happened for both ϕV and ϕK_S. The minima, close to 10%, should correspond to highest solvation and the maxima and at about 30%, to lowest solvation; the small ϕK_s and ϕV values denote that solvation is greater for 40-50% ethanol than for lower ethanol concentration. The large ϕV and ϕK_S and small denaturation ΔS^0_{cal} values calculated for poly(rA)·poly(rU) and ct-DNA compared to $[poly(dA\text{-}dT)]_2$ (Table 1) allows one to conclude that the solvation sequence is poly(rA)·poly(rU) < ct-DNA < $[poly(dA\text{-}dT)]_2$.

Together with the polynucleotide, the ethanol/water interactions play a prominent role. Ethanol–water presents abnormal behaviour of the ethanol partial molar volume,[43] chemical shift of hydroxyl signals of water[44] and adiabatic compressibility;[45] such abnormalities are regarded as structural in origin. Relaxation dielectric measurements by Sato et al.[10] had clarified the dynamics of the ethanol-water structure, calculating the activation enthalpy, entropy and free energy for ethanol-water as well as the contributions to partial

molar excess activation free energy, enthalpy, and entropy for water and ethanol. The concentration dependence of these quantities reveals two regions bound at 41%v/v ethanol (mole fraction x = 0.18); the excess properties adopt nearly zero value for x ~ 0.18, meaning that ethanol retains in the mixture nearly the same environment as in pure ethanol, forming chain-like clusters surrounded by water molecules. In the water-rich region, the excess properties exhibit two sharp maxima at x = 0.04 (11% v/v) and x = 0.08 (21% v/v), ascribed to structural enhancement of the H-bonding network of water by ethanol (hydrophobic hydration). For low ethanol concentration (x ~ 0.05), the ethanol molecules are essentially dispersed and surrounded by water molecules and come into contact only when the water available is insufficient to provide clathrate cavities for all ethanol molecules, thus stressing the role of the ethanol/water structure in the stability of nucleic acids.[46] The properties shown in Fig. 5 reflect the complex ethanol/water structure, for which changes in regions close to the critical points (excluding cubic expansion coefficint) were observed.

Viscosity. The average free energy of activation of viscous flow of a solute in solution, $\Delta\mu^{0,\neq}$, can be calculated as:[48]

$$\eta = \left(\frac{hN_A}{V_0}\right)\cdot \exp\left(\frac{\Delta\mu^{0,\neq}}{RT}\right) \qquad (11)$$

where V_0 represents the average molar volume of the aquo-organic solution, R is the gas constant, h is Plank constant and N_A is Avogadro constant. Table S21 lists the η_0 values for 0–50 % ethanol/water mixtures and 25-65 ºC. The $\ln\eta_0$ versus $1/T$ linear plot (Fig. 6) yields $\Delta\mu^{0,\neq}/R$ and ln (hN_A/V_0) (Table 2). Relative viscosities (η/η_0) serve to characterize the viscosity behaviour of DNA.[47] Figs. 6S and 7S show the variation of viscosity and relative viscosity with the ethanol concentration at different temperatures. For low alcohol content (x < 20%), the relative viscosities calculated were close to those of aqueous DNA.

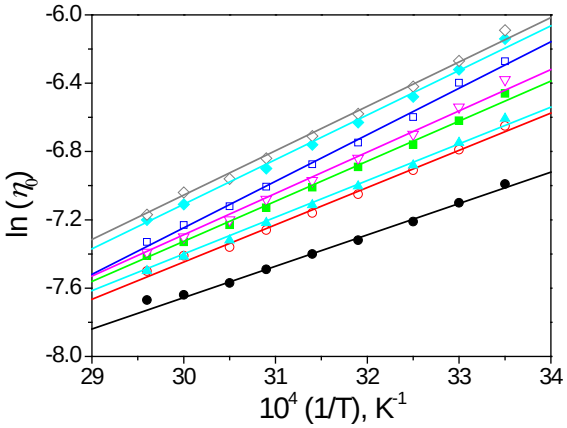

Fig. 6 ln η_0 versus $1/T$ plot as a function of ethanol/water mixtures: (●) 0, (○)10, (▲)15, (■)20, (▽)25, (□)30, (♦)40 and (◊)50% (v/v) EtOH. Solid lines are the log fitting of eqn (11)

Fig. 7 shows the temperature effect on the relative viscosity η/η_0 for 20%(v/v) ethanol/water. The behaviour was as expected,[11] except for $[poly(dA\text{-}dT)]_2$ which showed a transition close to the denaturation temperature for each ethanol/water mixture; the $T_{m,vis}$ values concur with the spectroscopic, $T_{m,sp}$, and calorimetric, $T_{m,cal}$, values (Table 1 and Figure 3B); similar behaviour has been reported earlier for other polynucleotides.[47] It should be stressed that, whereas η relies on T, the relative viscosity, η/η_0, does not, except when double-to-single transitions are observed (Figure 7).

Table 2 Values of $\Delta\mu_0^{0,\neq}$ and $V_{0,0}$ of the neat solvent and $\Delta\mu^{0,\neq}$ and V_0 values for RNA and DNA obtained with eqn (11) from viscosity data.

% (v/v) EtOH			$[poly(dA\text{-}dT)]_2$				ct-DNA		poly(rA)·poly(rU)	
			Single strand		Double strand					
	$\Delta\mu_0^{0,\neq}$ (kJ mol^{-1})	$V_{0,0}$ (cm^3 mol^{-1})	$\Delta\mu^{0,\neq}$ (kJ mol^{-1})	V_0 (cm^3 mol^{-1})	$\Delta\mu^{0,\neq}$ (kJ mol^{-1})	V_0 (cm^3 mol^{-1})	$\Delta\mu^{0,\neq}$ (kJ mol^{-1})	V_0 (cm^3 mol^{-1})	$\Delta\mu^{0,\neq}$ (kJ mol^{-1})	V_0 (cm^3 mol^{-1})
0	15	210	---	---	17	290	15	145	13	107
10	18	477	---	---	19	493	18	464	16	268
15	18	420	14	68	22	1212	---	---	---	---
20	20	693	19	449	24	3126	21	985	20	785
25	20	836	21	933	27	10017	---	---	---	---
30	23	1991	21	899	28	16258	23	2196	21	1235
40	22	1237	22	1121	31	42156	25	3323	23	1872
50	22	1123	---	---	---	---	24	2958	---	---

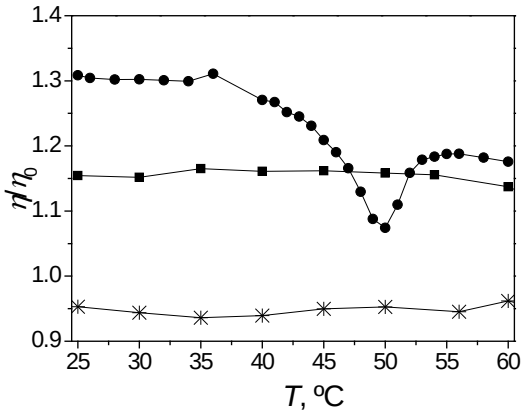

Fig. 7 Relative viscosity η/η_0 as a function of temperature: (■) ct-DNA, (●) $[poly(dA{-}dT)]_2$ and (∗) poly(rA)·poly(rU). 20%(v/v) ethanol, scan rate = 0.1 ºC/min, $C_P = 5\times10^{-4}$ M_{BP}, I = 0.1 M (NaCl), pH = 7.0.

For $[poly(dA\text{-}dT)]_2$, the η/η_0 versus T plot yields two regions, which were analyzed separately according to Eyring plot (Fig. 8); the first stretch, for temperatures above the melting point, provides information about the rheological properties with the simple helix, whereas the second, below $T_{m,vis}$, informs of the properties of the double helix.

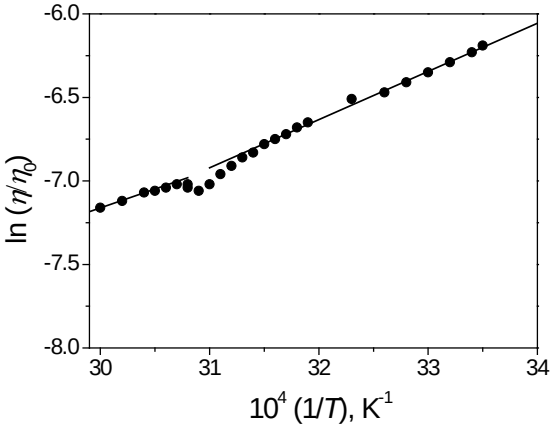

Fig. 8 Variation of the $\ln(\eta/\eta_0)$ as a function of inverse of temperature for $[poly(dA\text{-}dT)]_2$ at 20% (v/v) EtOH, $C_P = 5\times10^{-4}$ M_{BP}, I = 0.1 M (NaCl), pH = 7.0. Solid line is the linear fitting.

Application of eqn (11) to ct-DNA and poly(rA)·poly(rU) yielded single linear stretchs (Fig. 7S). Table 2 lists the V_0 and $\Delta\mu^{0,\neq}$ values calculated for ct-DNA, $[poly(dA\text{-}dT)]_2$ (single and double strand) and poly(rA)·poly(rU) for the ethanol-water mixtures. Both the activation energy of viscous flow and the average molar volume increased as the ethanol content was raised, consistent with ethanol-water mixed solvation spheres. V_0 was much higher for the

double-helix $[poly(dA\text{-}dT)]_2$ than for poly(rA)·poly(rU), ct-DNA adopting intermediate values. It must be recalled here that the A conformation of RNA is less solvated that the B conformation of DNA.

4. Conclusions

Thermal denaturation strongly relies on the A or B conformation of the polynucletide, ethanol and polynucleotide concentrations, ethanol/water structure and H-bonding. Below 30% ethanol, the denaturation temperature decreased for $[poly(dA\text{-}dT)]_2$ and ct-DNA, whereas for poly(rA)·poly(rU) it always increased due to aggregation. For $[poly(dA\text{-}dT)]_2$, the relative viscosities disclose transitions not observed for poly(rA)·poly(rU) and ct-DNA. The solvation is highest up to 10%, whereas the trend reversed the order up to 30%; for 40-50%, the solvation increased again. These critical points bear relation with the properties of ethanol/water and with the type of polynucleotide. In the water-rich region, the excess properties exhibit sharp maxima at 10% v/v and 20% v/v, ascribed to enhancement of the H-bonding network of water by ethanol (hydrophobic hydration). The solvation sequence followed the sequence: poly(rA)·poly(rU) < ct-DNA < $[poly(dA\text{-}dT)]_2$.

Associated Content

† **Electronic Supplementary Information (ESI) available**: Supporting Information for this article, Fig. 1S to 7S and Tables S1 to S21. See DOI:

Author Information

Corresponding Author
*Tel.: +34 947 258819, fax: + 34 947 258831. Email: begar@ubu.es
Universidad de Burgos, Departamento de Química
09001 Burgos, Spain

Acknowledgment

The financial support by Junta de Castilla y León (Fondo Social Europeo, project BU-

299A12-1) and Obra Social "la Caixa" project OSLC-2012-007, Spain, are gratefully acknowledged.

References

1 J. R. Wenner and V. A. Bloomfield, *J. Biomol. Struct. Dyn*., 1999, **17**, 461–471.

2 W. Saenger, *Principles of Nucleic Acid Structure*, Ed. Springer-Verlag, New York, 1988.

3 E. V. Frisman, A. N. Veselkov, S. V. Slonitsky, L. S. Karavaev and V. I. Vorob'ev, *Biopolymers*, 1974, **13**, 2169−2178.

4 G. Baldini and G. Varani, *Biopolymers*, 1986, **25**, 2187–2208.

5 G. Varani, L. Della Torre and G. Baldini, *Biophys. Chem.*, 1987, **28**, 175–181.

6 E. Grueso, F. Sanchez, V. I. Martin, E. García-Fernandez and R. Prado-Gotor, *Chem. Phys.*, 2008, **352**, 306–310.

7 B. Garcia, J. M. Leal, R. Ruiz, T. Biver, F. Secco and M. Venturini, *J. Phys. Chem. B*, 2010, **114**, 8555–8564.

8 X. Qu and J. B. Chaires, *J. Am. Chem. Soc*., 2001, **123**, 1–7.

9 N. N. Degtyareva, B. D. Wallace, A. R. Bryant, K. M. Loo and J. T. Petty, *Biophys. J*., 2007, **92**, 959–965.

10 T. Sato, A. Chiba and R. Nozaki, *J. Chem. Phys*., 1999, **110**, 2508−2521.

11 S. Song and C. Peng, *J. Dispersion Sci. Technol*., 2008, **29**, 1367−1372.

12 S. Y. Noskov, G. Lamoureux and B. Roux, *J. Phys. Chem. B*, 2005, **109**, 6705−6713.

13 T. T. Herskovits, S. J. Singer and E. P. Geiduschek, *Arch. Biochem. Biophys*., 1961, **94**, 99−113.

14 T. T. Herskovits, *Arch. Biochem. Biophys*., 1962, **97**, 474−484.

15 J. Piskur and A. Rupprecht, *FEBS Lett*., **1995**, 375, 174−178.

16 D. M. Gray, S. P. Edmondson, D. Lang and M. Vaughan, *Nucleic Acids Res.*, 1979, **6**, 2089−2107.

17 V. N. Potaman, Y. A. Bannikov and L. S. Shlyachtenko, *Nucleic Acids Res*., 1980, **8**, 635−642.

18 H. T. Steely Jr., D. M. Gray, D. Lang and M. F. Maestre, *Biopolymers*, 1986, **25**, 91−117.

19 A. F. Usatyi and L. S. Shlyakhtenko, *Biopolymers*, 1974, **13**, 2435−2446.

20 V. I. Ivanov, L. E. Minchenkova, A. K. Schyolkina and A. I. Poletayev, *Biopolymers*, 1973, **12**, 89−110.

21 J. T. Bokma, W. C. Johnson Jr. and J. Blok, *Biopolymers*, 1987, **26**, 893–909.

22 T. V. Chalikian and K. J. Breslauer, *Biopolymers*, 1998, **48**, 264−280.

23 T. V.Chalikian and R. B. Macgregor, *Phys. Life Rev*., 2007, **4**, 91−115.

24 T. V. Chalikian, J. Völker, A. R. Srinivasan, W. K. Olson and K. J. Breslauer, *Biopolymers*, 1999, **50**, 459–471.

25 G. Onori, A. Santucci, *J. Mol. Liq*., 1996, **69**, 161–181.

26 M. E. Reichmann, S. A. Rice, C. A.Thomas and P. Doty, *J. Am. Chem. Soc*., 1954, **76**, 3047–3053.

27 D. P. Remeta, C. P. Mudd, R. L. Berger and K. J. Breslauer, *Biochemistry*, 1993, **32**, 5064–5073.

28 G. C. Benson and O. Kiyohara, *J. Solution Chem*., 1980, **9**, 791-803.

29 D. D. Perrin and B. Dempsey, *Buffers for pH and Metal Ion Control*, Chapman and Hall, London, Wiley, New York, 1974.

30 M. Vorlícková, P. Sedlácek, J. Kypr and J. Sponar, *Nucleic Acids Res*., 1982, **10**, 6969−6979.

31 D. M. Gray and R. L. Ratliff, *Biopolymers*, 1975, **14**, 487−498.

32 J. L. Mergny and L. Lacroix, *Oligonucleotides*, 2003, **13**, 515−537.

33 V. V. Anshelevich, A. V. Vologodskii, A. V. Lukashin, M. D. Frankkamenetskii, *Biopolymers*, 1984, **23**, 39–58.

34 A. Marini, A. Muñoz-Losa, A. Biancardi and B. Menucci, *J. Phys. Chem. B*, 2010, **114**, 17128–17135

35 D. Jose and D. Porschke, *J. Am. Chem. Soc*., 2005, **127**, 16120-16128.

36 S. Beneventi and G. Onori, *Biophys. Chem.*, 1986, **25**, 181–190.

37 O. Kratky, H. Leopold, and H. Stabinger, *Methods Enzymol*., 1973, **27**, 98–110.

38 A. P. Sarvazyan, *Annu. Rev. Biophys. Biophys. Chem*., 1991, **20**, 321–342.

39 V. A. Buckin, *Mol. Biol.* (USSR), 1987, **21**, 615–629.

40 L. Lavelle and J. R. Fresco, *Biophys. Chem*., 2003, **105**, 701–720 and references therein.

41 A. Tikhomirova and T. V. Chalikian, *J. Mol. Biol.*, 2004, **341**, 551–563.

42 T.V. Chalikian, *J. Phys. Chem. B*, 1998, **102**, 6921–6926.

43 F. Franks and D. J. G. Ives, *Quart. Rev*., 1966, **20**, 1–44.

44 A. Coccia, P. L. Indovina, F. Podo and V. Viti, *Chem. Phys*., 1975, **7**, 30–40.

45 S. V. Paston, I. M. Zyryanova, Y. V.Zaichikova and V. V. Zamotin, *J. Struct. Chem*., 2007, **48**, 734–739.

46 G. Onori, *J. Chem. Phys*., 1988, **89**, 4325–4332.

47 C. R. Cantor and P. R. Shimmel, *Biophysical Chemistry*. a) *Part III: The behaviour of biological macromolecules*, pg 1222. b) *Part II: Thechniques for the study of biological structure and function*, chapter 12. W. H. Freeman and Company, New York, 1980.

48 S. Marchetti, S. Cinelli and G. Onori, *Chem. Phys. Lett*., 2010, **493**, 158–164.